Chemistry & Biology
Article

Utilization of an In Vivo Reporter for High Throughput Identification of Branched Small Molecule Regulators of Hypoxic Adaptation

Natalya A. Smirnova,[1] Ilay Rakhman,[1] Natalia Moroz,[1] Manuela Basso,[1] Jimmy Payappilly,[1] Sergey Kazakov,[2] Francisco Hernandez-Guzman,[3] Irina N. Gaisina,[4] Alan P. Kozikowski,[4] Rajiv R. Ratan,[1,*] and Irina G. Gazaryan[1,*]
[1]Burke Medical Research Institute, Department of Neurology and Neuroscience, Weill Medical College of Cornell University, 785 Mamaroneck Ave, White Plains, NY 10605, USA
[2]Department of Chemistry and Physical Sciences, Pace University, 861 Bedford Road, Pleasantville, NY 10570, USA
[3]Accelrys Inc., 10188 Telesis Ct. Suite 100, San Diego, CA 92121, USA
[4]Department of Medicinal Chemistry and Pharmacognosy, University of Illinois at Chicago, 833 South Wood Street, Chicago, IL 60612, USA
*Correspondence: igazarya@burke.org (I.G.G.), rratan@burke.org (R.R.R.)
DOI 10.1016/j.chembiol.2010.03.008

SUMMARY

Small molecules inhibiting hypoxia inducible factor (HIF) prolyl hydroxylases (PHDs) are the focus of drug development efforts directed toward the treatment of ischemia and metabolic imbalance. A cell-based reporter produced by fusing HIF-1α oxygen degradable domain (ODD) to luciferase was shown to work as a capture assay monitoring stability of the overexpressed luciferase-labeled HIF PHD substrate under conditions more physiological than in vitro test tubes. High throughput screening identified novel catechol and oxyquinoline pharmacophores with a "branching motif" immediately adjacent to a Fe-binding motif that fits selectively into the HIF PHD active site in in silico models. In accord with their structure-activity relationship in the primary screen, the best "hits" stabilize HIF1α, upregulate known HIF target genes in a human neuronal line, and exert neuroprotective effects in established model of oxidative stress in cortical neurons.

INTRODUCTION

Hypoxia is a common etiology of cell injury in human disease, including stroke, myocardial infarction, and solid tumors. Over the past two decades, cell adaptation to hypoxia has emerged as a well-defined active process. Each cell of a multicellular organism can respond to hypoxia by building up hypoxia inducible factor (HIF), a ubiquitous transcription factor capable of activating a battery of genes including genes involved in glucose uptake and metabolism, extracellular pH control, angiogenesis, erythropoiesis, mitogenesis, and apoptosis. The discovery of HIF opened new horizons for the treatment of ischemia and cancer: upregulation of HIF levels has been shown to be beneficial for ischemic diseases, stem cell proliferation (Zhang et al., 2006), and transplantation (Liu et al., 2009), whereas downregulation of elevated HIF, a marker of most aggressive cancers, represents a new approach for cancer treatment.

HIF consists of two subunits, HIF-1α and HIF-1β; HIF-1α is rapidly degraded under normoxic conditions, whereas HIF-1β is stable (Wang et al., 1995; Wang and Semenza, 1995). HIF levels are regulated primarily by posttranslational modification of conserved proline residues. Hydroxylation of Pro564 and/or 402 residues in HIF-1α is a prerequisite for its interaction with the von Hippel-Lindau (VHL) protein yielding a complex that provides HIF ubiquitinylation and subsequent proteasomal degradation (Kaelin, 2005). Hydroxylation of Pro564 occurs prior to Pro402 (Chan et al., 2005), though some experiments contradict this finding (Villar et al., 2007). Hydroxylation of HIF-1α Asn803 blocks its interaction with transcriptional proactivator p300 (Lando et al., 2002). In both cases HIF hydroxylation is executed by α-KG dependent non-heme iron dioxygenases, HIF prolyl-4-hydroxylase (PHD1-3 isozymes) and asparaginyl hydroxylase (or the so-called FIH, factor inhibiting HIF) (Hirota and Semenza, 2005).

HIF1 also upregulates a number of prodeath proteins, and thus HIF1 upregulation can be either prodeath or prosurvival. However, recent evidence (Siddiq et al., 2005; Knowles et al., 2004; Baranova et al., 2007) strongly suggests that PHDs and FIH are important targets for medical intervention for a number of conditions, including chronic anemia and stroke. PHD inhibitors abrogate the ability of HIF1-mediated transactivation of BNIP3 and PUMA to potentiate oxidative death in normoxia (Aminova et al., 2008). Although new targets for intervention in the HIF pathway are constantly emerging, the latter observation justifies the search for PHD inhibitors rather than for other types of HIF activators. New substrates have been recently identified for PHD1 (e.g., Rpb1, large subunit of RNA polymerase II [Mikhaylova et al., 2008]) responsible for the fundamental enzymatic activity of the complex, synthesizing all cellular mRNAs) and PHD3 (e.g., β_2-adrenergetic receptor [Xie et al., 2009], whose sustained downregulation is associated with heart failure and asthma) placing HIF PHDs into the focus of drug development efforts. Despite characterization of HIF PHDs as a potential target for anti-ischemic therapy, few high throughput screening (HTS) results for PHD inhibitors are publically available.

In this work, we developed a novel application for an approach elegantly validated by Kaelin and Livingston's group for visualization of HIF stabilization in transgenic mice (Safran et al., 2006) and used it for the purposes of HTS. The reporter system

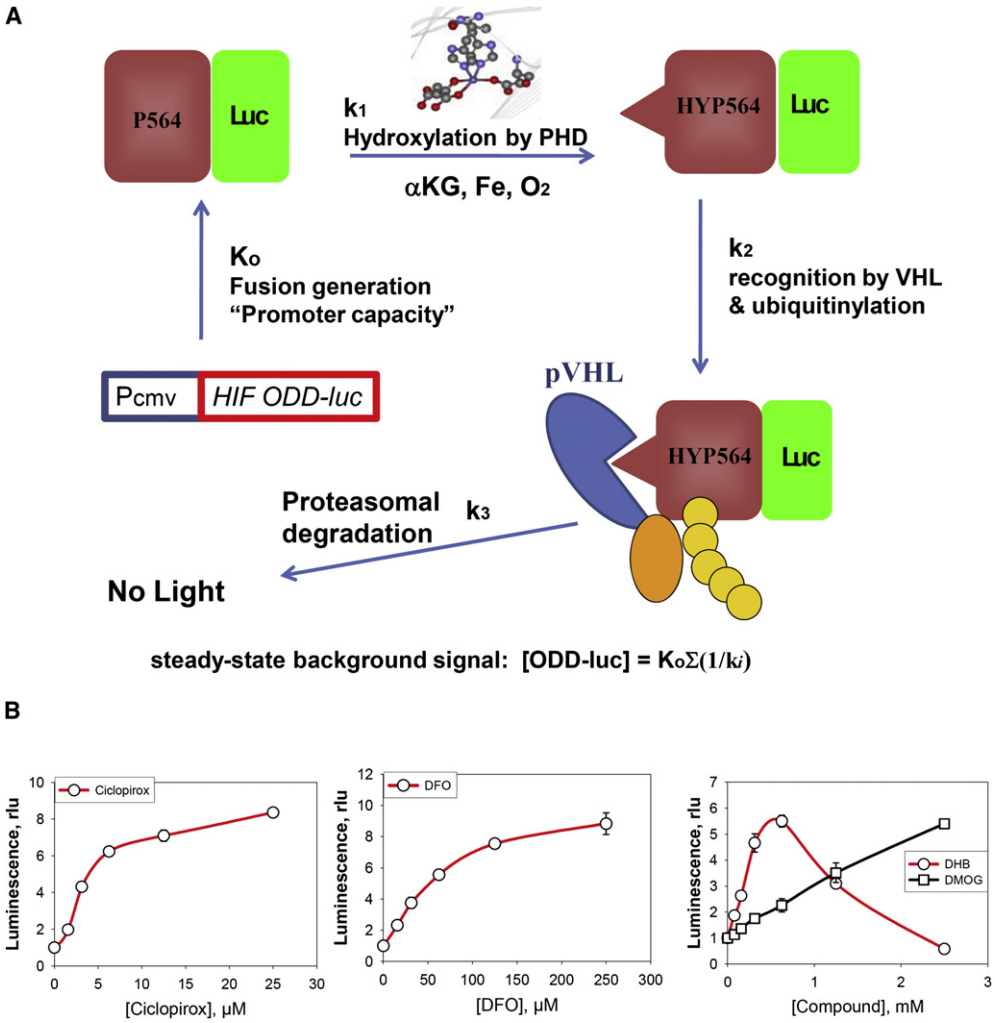

Figure 1. Mechanism of Reporter Activation and Response to Canonical HIF PHD Inhibitors

(A) Schematic presentation of reporter performance showing key steps/potential sites of inhibition.

(B) Reporter response to canonical HIF PHD inhibitors: ciclopirox, DFO, DMOG, and DHB.

All values are presented as mean ± SEM. Calculation of activation parameters from the titration curve in shown in Figure S1.

consists of the HIF-1α gene fragment encoding the oxygen degradable domain (ODD) containing the key proline residue followed by luciferase gene (*luc*). The regulation of luciferase protein stability in this reporter system is the same as the physiological activation of HIF: hydroxylation of oxygen-degradable domain (ODD, which contains 530-653 amino acids [aa] of HIF1-α) results in recognition of the ODD-luc fusion protein by VHL followed by its ubiquitinylation and proteasomal degradation (Figure 1A), and as we present below, the approach proved to be productive for HTS purposes.

We performed a cell-based HTS of 85,000 compounds for HIF protein stabilizers to identify those working as specific HIF PHD inhibitors. The most intriguing finding from the primary screen of 85,000 compounds was the group of branched 8-hydroxyquinoline derivatives whose binding mode into the active site of PHD2 resembles that of the HIF peptide. The biological effects of the newly identified hits—i.e., HIF1 protein stabilization, induction of HIF1-regulated genes such as vascular endothelial growth factor (VEGF), lactate dehydrogenase (*LDHA*), and phosphoglycerate kinase 1 (*PGK1*), neuroprotection in homocysteic acid (HCA) cellular model of oxidative stress—are in good agreement with their activation effects in the reporter assay.

RESULTS

Development and Optimization of the ODD-luc Reporter System

The reporter cell lines constitutively expressing ODD-luc (human neuroblastoma, SH-SY5Y) were stable for more than 1 year without significant change in their response to canonical PHD inhibitors such as deferoxamine (DFO), dihydroxybenzoate (DHB), dimethyloxalylglycine (DMOG), and ciclopirox (Figure 1B). The dependence of the ODD-luc reporter signal on inhibitor concentration has a sigmoid shape (Figure 1B and Figure S1 available online), which is characterized by maximum activation, IC_{50} and a "concentration lag," which likely reflects the presence

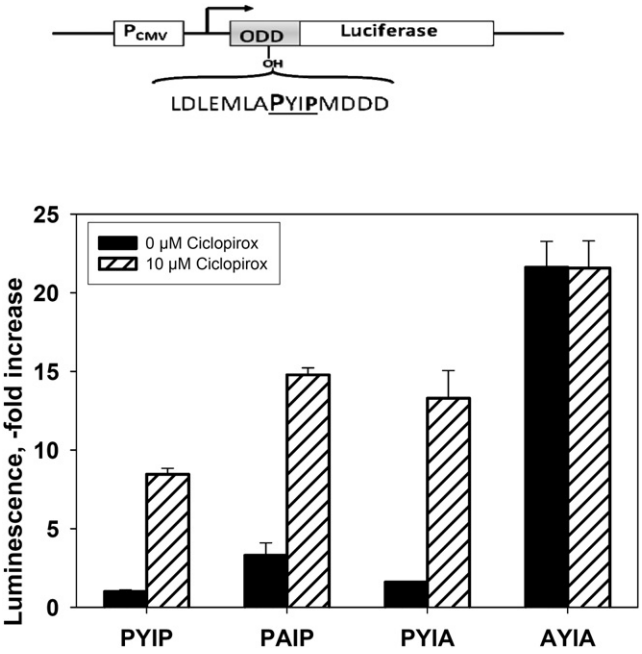

Figure 2. Effect of Mutations Adjacent to Pro564 on the Reporter Response to 10 μM Ciclopirox upon 3 hr Incubation

PHD1 and PHD2 are supposed to be the major HIF PHD isoforms present in neuroblastoma cell line as judged by PCR (Figure S2). All values are presented as mean ± SEM.

of iron in the media, which can bind drug and delay or impede its intracellular effects. The concentration of iron in the serum used for neuroblastoma cultivation is 1.5 μM.

In order to verify the specificity of luciferase changes as an assay for PHD activity, several control lines were developed: the control line expressing ODD-luc with proline 564 and 567 mutated to Ala generates luciferase fusion that cannot be degraded and experimentally identifies a ceiling level of ODD-luc protein attainable in these cells. The background signal for the wild-type HIF ODD-luc line (PYIP) corresponds to approximately 5%–6% of the ODD-luc levels in the control line AYIA (double mutant P564A/P567A line) (Figure 2). Treatment with 10 μM ciclopirox results in a 10-fold increase of a background signal for the wild-type ODD-luc reporter (PYIP line), i.e., reaches almost 50% of the threshold value (Figure 2). These particular conditions are ideal for HTS because they promote the selection of both weaker and more potent inhibitors than ciclopirox.

The neuroblastoma cell line expresses all three PHD isoforms (Figure S2). In the second control line, as an initial test of fidelity of our constructs for reporting endogenous regulation, we mutated Tyr565 to Ala, which has been previously shown to decrease the affinity of HIF for PHD2 (Landazuri et al., 2006; Bruick and McKnight, 2001; Jaakkola et al., 2001). As expected, line PAIP shows a 3-4-fold higher steady-state level of ODD-luc than the wild-type line (Figure 2). Of note, the third control, mutation of Pro567 to Ala, which has been shown to influence recognition of the HIF ODD by PHD3 (Landazuri et al., 2006), has lesser effect on ODD-luc levels (Figure 2). The fact that the reporter system is sensitive to single-point mutations surrounding Pro564 region in accord with previously published observations (Landazuri et al., 2006; Bruick and McKnight, 2001; Jaakkola et al., 2001) provides evidence that the rate-limiting step is controlled by the PHD catalyzed reaction.

The HIF ODD-luciferase reporter system is controlled by the rate of PHD-catalyzed reaction, and from an enzyme kinetics point of view it is a "capture assay" monitored by the consumption of a substrate, the heterologously expressed HIF ODD-luciferase fusion protein. In the kinetic regimen, i.e., monitoring the time course of luminescence changes (Figure 3A), the ODD-luc reporter system permits quantitative characterization of promoter capacity (K_o, rate of fusion protein generation), enzyme activity, and inhibition constant determination.

The rate of fusion accumulation equals to the rate of its production (K_o) minus the rate of rate-limiting step, controlled by HIF PHDs, which obeys Michaelis-Menten kinetics, as follows:

$$v = d[ODDluc]/dt = K_0 - k_1[PHD][ODDluc]/\{K_m(1 + [I]/K_i) + [ODDluc]\} \quad (1)$$

where K_m is the inhibition constant for a competitive inhibitor, k_1 is the rate coefficient, and [PHD] and [ODD-luc] are the concentrations of the enzyme and substrate, respectively.

The background luminescence signal calibrated with recombinant luciferase allows us to estimate the steady-state concentration of the ODD-luc fusion protein. Under the conditions used the steady-state value of 60 rlu (relative light units) corresponds to 1 pg luciferase protein; dividing this number by the total cell volume taken as a single cell volume (233 μ^3) multiplied by 30,000 cells/well density (number of cells in a 96-well dish), we get the ODD-luc fusion protein steady-state concentration equal to 2.3 nM, which is way below all reported K_m values for HIF1 (Tuckerman et al., 2004; Koivunen et al., 2006; Hewitson et al., 2007; Dao et al., 2009). Therefore, we work under nonsaturating conditions with respect to HIF substrate, i.e., optimal conditions for selecting inhibitors competitive against HIF substrate. Moreover, as compared with the in vitro assay, which uses a 19 amino acid peptide fragment surrounding the hydroxylated proline (P564), our ODD-luciferase construct contains 123 amino acid acids, and thus more closely emulates the behavior of native HIF. We can consider the initial concentration of fusion much lower than K_m and ignore it in the rate equation:

$$v = d[ODDluc]/dt = K_0 - k_1[PHD][ODDluc]/K_m(1 + [I]/K_i). \quad (2)$$

Knowing the capacity of the promoter, we can determine the inhibition constant, but not the inhibition type, from the initial rates of signal accumulation at varied fixed concentrations of potential inhibitor. The capacity of promoter K_0 can be determined under the conditions of total inhibition of PHD activity by means of complete iron deprivation achieved in the presence of high concentrations of ciclopirox, i.e., when the increase in the ciclopirox concentration gives no further increase in the rate of luciferase signal growth (Figure 3B). The intracellular enzyme activity (k_1[PHD]/K_m) can be also determined by dividing the rate of fusion protein accumulation by the steady-state concentration of the fusion protein determined directly from one and the same experiment in luciferase units, without recalculation for the cellular volume, and corresponds to 0.05 min^{-1}. The linear plot of 1/(K_0 – v) versus the inhibitor concentration

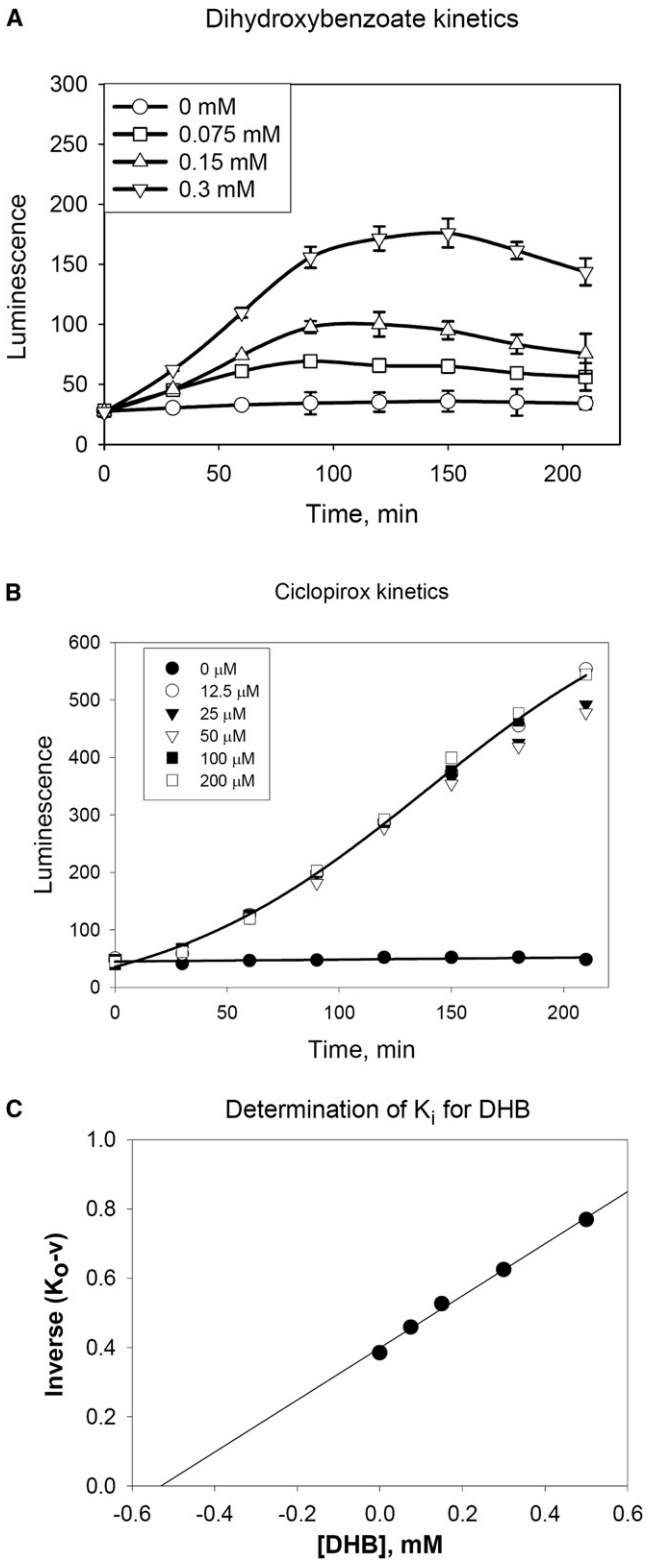

Figure 3. Determination of Apparent HIF PHD Inhibition Constants from Time Course of Reporter Activation

(A and B) Original kinetic curves for DHB (A; all values are presented as mean ± SEM) and ciclopirox (B).

(C) Linear plot to calculate the apparent inhibition constants using Equation 3.

gives the value of the apparent inhibition constant as the intercept on *x* axis (Figure 3C):

$$1/(K_0 - v) = K_m(1 + [I]/K_i)/k_1[PHD][ODDluc]_0. \quad (3)$$

The apparent inhibition constant determined for DHB and DMOG is 0.52 mM and 1.3 mM, respectively, which is in agreement with previous observations on their biological effects exerted in the millimolar range (Philipp et al., 2006; Asikainen et al., 2005; Lomb et al., 2009) and IC_{50} reported for PHD2 in vitro assay (Cho et al., 2005).

The response of the ODD-luc reporter to canonical HIF PHD inhibitors, and the increased stability of single-point mutant reporters in accord with the predictions, provided confidence that this system could be utilized for screening for novel small molecule HIF PHD inhibitors; hence, we then set out to optimize conditions for high throughput screening (see Experimental Procedures).

A Primary Screen Identified 160 Validated Hits

The screen of an 85,000 compound library (including those from Spectrum, ChemDiv, AMRI, ChemBridge. Prestwick, and Cerep) resulted in 295 hits, among which 160 were confirmed in follow up testing. Of note, no established proteasomal inhibitors were identified in the screen. Hits were then classified into 10 structural clusters, 6 of which are shown in Figure 4A.

Hydrazides and Hydrazones

Among this chemical group (55 hits of 76 hydrazides and hydrazones tested) are well-established HIF activators (Almstead et al., 2002) that form a tight 2:1 6-cordinated Fe complex in solution but not within the enzyme. It is likely that global cellular iron deprivation emerging from these compounds results in reporter activation comparable or even higher than that for ciclopirox. Interestingly, we identified a group of edaravone hydrazone derivatives that can provide only two iron ligands, such as (*Z*)-1,3-diphenyl-4-(thiazol-2-yl-hydrazono)-1*H*-pyrazol-5(4*H*)-one (**I**) (Figure 4A) and (*Z*)-4-(benzo[*d*]thiazol-2-yl-hydrazono)-1,3-diphenyl-1*H*-pyrazol-5(4*H*)-one, and unlike other members of the class that bind iron outside the enzyme, these may coordinate iron inside the enzyme. However, the level of reporter activation for the two iron ligand edaravone derivatives is lower (86% and 70%, respectively) than for hydrazones providing three iron ligands (above 100%). Of note, edaravone has been used in Japan to treat humans with stroke (Kikuchi et al., 2009a, 2009b). However, edaravone itself does not provide iron ligands and shows no reporter activation.

Hydralazine, an FDA-approved antihypertensive agent, is known to be a HIF stabilizer (Knowles et al., 2004; Michels et al., 2009) and an activator of a hypoxia response element (HRE)-luc reporter (Ratan et al., 2005). Our data also implicate a hydralazine analog, (2-hydrazinyl-4,6-diphenylpyrimidine) (**II**) (Figure 4A) as a potent HIF stabilizer (64% or 6.7-fold activation). The presence of a terminal amino group and free rotation of phenyl rings (*ortho*-hydroxy group in one ring abolishes activation effect) are required for the activation effect observed. The compound exhibits no iron chelation properties in solution.

Dibenzoylmethanes

We identified two compounds which exhibit a similar docking mode to DBM, another established HIF activator (Mabjeesh

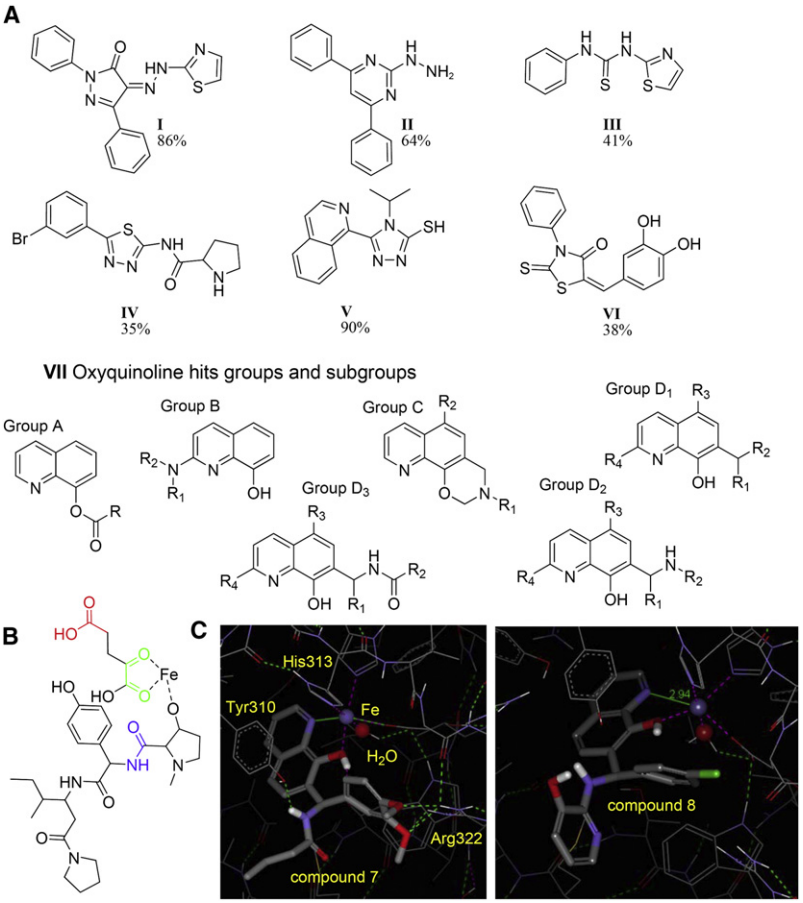

Figure 4. New Hit Groups Identified in HTS

(A) Chemical structures of hits: (**I**), Edaravon-type hit: (*Z*)-1, 3-diphenyl-4-(thiazol-2-yl-hydrazono)-1*H*-pyrazol-5(4*H*)-one (86%); (**II**), Hydralazine type hit: 2-hydrazinyl-4,6-diphenylpyrimidine (64%); (**III**), Dibenzoylmethane group hit: 1-phenyl-3-(1,3-thiazol-2-yl)thiourea (41%); (**IV**), Thiadiazole group hit: *N*-[5-(3-bromophenyl)-[1,3,4]thiadiazol-2-yl]pyrrolidine-2-carboxamide (35%); (**V**), Triazole group hit: 4-isopropyl-5-isoquinolin-1-yl-4*H*-[1,2,4]triazole-3-thiol (90%); (**VI**), Catechol group hit: (*E*)-5-(3,4-dihydroxybenzylidene)-3-phenyl-2-thioxothiazolidin-4-one (38%); docking of branched catechol hits is shown in Figure S3.

(B) Schematic presentation of docking mode of hydroxylated HIF peptide into PHD2.

(C) Docking of best hits, compounds **7** and **8**, into PHD2.

et al., 2003). The sulfur-containing analog of DBM (**III**) (Figure 4A) resulted in a 5-fold (or 41% of ciclopirox) reporter activation.

Thiadiazoles

Thiadiazole compounds (four hits out of eight compounds tested) provide modest activation (3-5-fold activation or 25%–40% of the internal standard, Figure 4A, **IV**) and have a number of potential iron ligands that may support two modes of the compound docking into the PHD2 active site in place of αKG. In either case, the predicted interference from "bulky" attachments at the amide end is in agreement with experimental observations: 2-amino-*N*-(5-(4-bromophenyl)-[1,3,4]thiadiazol-2-yl)-3-methylpentanamide and 2-amino-*N*-(5-(4-methoxy-phenyl)-[1,3,4]thiadiazol-2-yl)-3-phenylpropanamide show no reporter activation at all.

Isoquinolinotriazolylthiols

This class of compounds likely stabilized ODD-luc in our assay via their iron chelation in solution. Iron chelation by isoquinolinotriazolylthiols (**V**) (Figure 4A) depends on their ability to provide two iron ligands and depends on the rotation restriction between isoquinoline and triazole rings. Activation drops by 3-fold with substitutions at position 4 of the thiazole ring and with bulky attachments like *meta*-, and *para*-substituted phenyl rings or benzyl substituent containing a methyl branch. Two of eight hits (5-isoquinolin-1-yl-4-(2-trifluoromethyl-phenyl)-4*H*-[1,2,4]triazole-3-thiol and 4-isopropyl-5-isoquinolin-1-yl-4*H*-[1,2,4]triazole-3-thiol (**V**) (Figure 4A) show reporter activation close to that for our internal standard, ciclopirox. The activation effects were consistent with the predicted substitution effects on iron chelation ability, therefore this group is likely to act through iron chelation rather than iron coordination in the active center.

Flavonoids are HIF activators (Wilson and Poellinger, 2002; Jeon et al., 2007), but their mechanism of action remained obscure and no structure-activity relationships (SAR) have been described for this class of compounds. The 85,000 compound library had 80 flavones (20 of which were hits), 90 isoflavones (7 of which were hits), and 16 flavanones (6 of which were hits). The SAR studies for flavone/isoflavone/flavanone family have been completed and structural requirements for optimal docking have been formulated. In particular, the absence of substitutions in the phenyl ring for 3-hydroxyflavone derivatives is a must for optimal docking and reporter activation, while the presence of hydroxy- or methoxy- groups in phenyl ring of 5-hydroxyflavones (as well as isolfavones and flavanones) is also a requirement for optimal docking and reporter activation.

Chalcones, precursors for flavones, were also hits in our screen (the best one is 2′β-dihydroxychalcone, showing 7.5-fold activation or 71%). All provide at least two iron ligands but are unlikely to be useful as biological tools or drugs because they show rather high toxicity compared with flavones. Of the active **coumarines** (2 active out of 36 tested), both contain a strong iron binding motif, vicinal hydroxyls, and are well-known for forming tight iron complexes. Their size allows binding inside the PHD active site, whereas coumarines with bulky attachments show no reporter activation.

Catechols

The catechol (3,4-dihydroxyphenyl) moiety was found in 100 compounds tested (excluding flavones and coumarins), however, only 8 among them were hits. Ethyl-3,4-dihydroxybenzoate is a known PHD inhibitor, which activated the reporter at concentrations 5-fold higher (>50 μM, see Figure 1B) than the standard screening concentration 10 μM. *L*-Dopa, but not *D*-dopa, carbidopa, dopamine, and other analogs tested, was a modest hit (21% or 3-fold reporter activation, IC_{50} = 15 μM). This finding is of potential interest given the recent data on increased

protective effects for Sinemet (combination of *L*-dopa and carbidopa) in Parkinson's disease. Thioxothiazolidinones (**VI**) (Figure 4A) exhibited rather modest reporter activation (35%–45% or 4-5-fold). Most intriguing was the identification of four hits containing a branching motif that in in vitro models, screens the entrance to the active site (two of them are shown in Figure S3).

Oxyquinolines (22 hits out of 66 compounds tested) could be classified into four groups, and among those one could be further divided into three subgroups (**VII A-D**, Figure 4A). Oxyquinoline derivatives are established inhibitors of HIF prolyl hydroxylase. They appear to act by providing two ligands for iron binding and thus inhibit PHD2 in vitro with an IC_{50} above 3 μM (Warshakoon et al., 2006d). Compounds from group **A**, such as chloroacetoquinoline, exhibit reporter activation comparable to 8-hydroxyquinoline itself (4-5-fold reporter activation or 35%–45%), and its halogenated derivatives such as iodoquinol, broxyquinoline, clioquinol (Choi et al., 2006), and chloroxine. Clioquinol is of particular interest given its established salutary effects in models of Alzheimer's disease and Huntington's disease and its serious consideration for late-stage human trials (Kaur et al., 2003; Adlard et al., 2008). For the oxyquinolines, the reporter signal drops with the increased size of the R group (see Table S1 available online). By contrast, we found that oxyquinoline derivatives containing a branched substitution at position 7 (**VII D,** Figure 4A), as well as their conformationally constraint analogs (group **C**) with reasonably short but flexible linkers, are the best compounds that result in reporter activation comparable or superior to ciclopirox (see Table S1). For optimal HIF activation, either halogen or NO_2 group at position 4 (R_3) is favorable, whereas any substitution at position 2 (group **B**) is not tolerated. The binding mode of hydroxylated HIF peptide (Figure 4B) gives a strikingly similar position of Tyr565 against αKG-binding plane to that of hydroxy-phenyl ring against the oxyquinoline plane in our best hit, compound **8** (Figure 4C), and this pushed us to study the effects of branched oxyquinolines in detail.

Structure-Activity Studies for Selected Branched Oxyquinolines

To explore a variety of our hits further, we had to develop a rationale to discriminate between specific inhibition of PHD and nonspecific iron chelation. We assume that if there is no specific interaction between the enzyme and iron-binding inhibitors, the enzyme inhibition constants (or in our case, IC_{50}) will change in parallel with the iron-binding constants. Specific inhibitors, i.e., those coordinating iron directly at the PHD active site, should deviate ("pop-up") from the group of iron chelators with the same affinity and exhibit better inhibition constants (IC_{50}) than those that simply bind iron. We determined the apparent iron binding constants in solution for a dozen of hits of interest (Table 1). In addition, we determined the rate constant for association from the kinetics of calcein displacement from its complex with iron (k_a), which characterizes how fast oxyquinoline binds iron (Table 1). The apparent iron binding constant K_{Fe} for the compounds studied varies more than one order of magnitude, from 0.08 to 2.0 μM, in parallel with the changes in the association rate constant (from 20 to 250 $M^{-1}s^{-1}$), while the dissociation rate constant is barely affected.

We can divide the studied oxyquinolines into three groups with respect to their iron binding ability: first, those close to that of ciclopirox (compounds **1**,**2**,**4**,**7**,**10**,**13**), second, similar to oxyquinoline (**6**,**8**,**11**,**12**), and third, very poor iron chelators (**3**,**5**,**9**) showing very poor reporter activation. The best inhibitors are found in the first two groups. Table 1 clearly points to five compounds as reporter activators better than ciclopirox: compound **8** belongs to D2 group, while all others (**1**,**4**,**6**,**7**) belong to D3 group. The comparison of iron binding and reporter activation parameters (Table 1) shows no direct correlation between chelation ability of oxyquinolines and IC_{50} for PHDs; the obvious requirements for good activation are the absence of 2-methyl group in oxyquinoline (R_4) and dioxol group in the phenyl ring R_1. The absence of a linker, i.e., immediately attached branched motif to the position 7 of oxyquinoline (**10**, Table 1), is good for iron chelation, but not for reporter activation. We conclude that structural determinants, but not iron binding constants, play a major role in reporter activation.

Biological Effects of Best Branched Oxyquinoline Hits

To verify that reporter activation corresponds to the biological effects exerted by branched oxyquinolines, we selected compounds **7** and **8** as positive controls, and oxyquinoline and compound **10** as negative controls. The reduced efficacy of compound **10** in the reporter assay is not related to poorer cell membrane permeability: indeed, compound **10** activates the reporter much faster than compound **7** (see kinetics of reporter activation for both compounds in Figure S4). As expected, the best hits (**7** and **8**), but not our negative controls (5 μM), significantly stabilized HIF1α protein (Figure 5A) in the SH-SY5Y human neuroblastoma cell line 3 hr after addition of the compounds to the bathing media. Accordingly, HIF1-regulated genes such as *Epo*, *VEGF*, *LDHA,* and *PGK1* (Figure 5B) were also induced by the small molecules that stabilized HIF-1α, although it is interesting to note that compound **7** and **8** activated distinct patterns of HIF-dependent gene expression, suggesting that these compounds may affect distinct HIF PHD isoforms.

Our prior studies on HIF PHD inhibition in glutathione depletion model of oxidative stress in cortical neurons revealed that inhibition of HIF PHD1 by gene silencing or with canonical PHD inhibitors such as DFO (iron chelator), DHB, and DMOG (αKG mimics) was sufficient to prevent cell death independent of HIF (Siddiq et al., 2009). The hits identified in HTS with HIF1 ODD-luc reporter are unlikely to be PHD-isoform specific, therefore, one may expect that they will target PHD1 as well and exert neuroprotection in the above model. As expected, compounds **7** and **8**, but not **10**, protect cortical neurons stimulated to die by depletion of the versatile antioxidant glutathione (Figure 6). Oxyquinoline and compound **10** are not only less potent HIF activators, but also 20-40 times less potent as neuroprotectants (Figure 6). Of note, compounds **7** and **8** possess an IC_{50} for neuroprotection an order of magnitude lower (0.25 μM) than those required for reporter and HIF stabilization (IC_{50} 2.0-2.5 μM). Thus, neuroprotection is exhibited in the nanomolar range only by the best hits, and, as one would predict from the reporter activation (Table 1), compound **7** is more potent than compound **8**. The inhibition of other enzymes of this class with the resolved crystal structure is ruled out due to the structural constraints

Table 1. Comparison of Reporter Activation Parameters and Iron-Binding Properties of Branched Oxyquinolines (Structural Subgroups D1-D3 as Depicted in Figure 4)

Compound Group and Number	Compound Structure	Maximum Activation (-fold)	IC_{50}, μM	"Lag," μM	K_{Fe}, μM	k_a, $M^{-1}s^{-1}$
Ciclopirox		8.5 ± 0.5	4.5 ± 0.5	2 ± 0.5	0.08 ± 0.02	300 ± 50
Oxyquinoline		4.5 ± 0.3	10 ± 1	4 ± 0.5	0.20 ± 0.05	110 ± 20
D1, #10	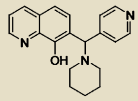	5.0 ± 0.4	10 ± 1	1.8 ± 0.2	0.08 ± 0.02	250 ± 50
D2, #9	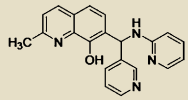	5.5 ± 0.5	10 ± 1	5 ± 0.2	0.78 ± 0.18	30 ± 5
D2, #12	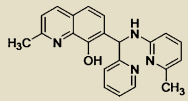	6.0 ± 0.5	4.5 ± 0.5	3 ± 0.4	0.20 ± 0.05	n.d.[a]
D2, #5	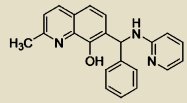	5.2 ± 0.3	7 ± 0.2	5 ± 0.5	1.50 ± 0.30	20 ± 3
D2, #8	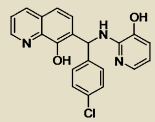	7.0 ± 0.2	2 ± 0.3	0.6 ± 0.1	0.19 ± 0.04	110 ± 20
D2, #3	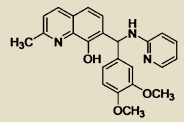	2.0 ± 0.3	12 ± 0.5	10 ± 0.5	0.80 ± 0.20	20 ± 3
D2, #13	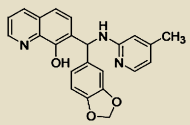	6.0 ± 0.2	7 ± 0.2	5 ± 0.5	0.10 ± 0.02	n.d.
D2, #2	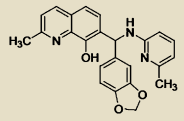	4.5 ± 0.5	12 ± 1	7 ± 0.5	0.10 ± 0.02	n.d.
D3, #1	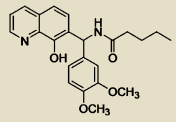	7.0 ± 0.2	2.6 ± 0.2	1 ± 0.1	0.11 ± 0.02	240 ± 40

Table 1. *Continued*

Compound Group and Number	Compound Structure	Maximum Activation (-fold)	IC_{50}, μM	"Lag," μM	K_{Fe}, μM	k_a, $M^{-1}s^{-1}$
D3, #4	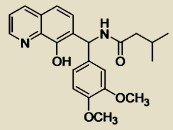	6.8 ± 0.2	2.1 ± 0.2	0.6 ± 0.2	0.10 ± 0.02	210 ± 40
D3, #7	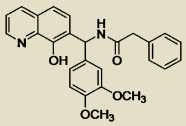	7.0 ± 0.2	2.2 ± 0.2	1 ± 0.1	0.10 ± 0.02	180 ± 35
D3, #6	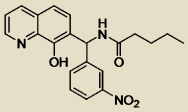	7.2 ± 0.3	4 ± 0.1	1.8 ± 0.2	0.20 ± 0.04	95 ± 15
D3, #11	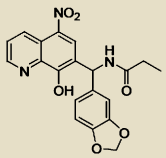	4.0 ± 0.3	12 ± 1	8 ± 1	0.15 ± 0.03	100 ± 20

[a] n.d. = not determined.

(Figure S5). These results support our conclusion that structural effects play a major role in reporter activation (and HIF stabilization) rather than common iron binding potency of the studied oxyquinolines. These studies are the first to use chemical tools to validate a role for HIF PHD inhibition and not iron chelation per se in stabilizing HIF and protecting neurons from oxidative death.

DISCUSSION

Two primary modes of screening for HIF activators have been well described: a recombinant enzyme-based screen for PHD2 inhibitors (used by Fibrogen [Ivan et al., 2002], Amgen [Tegley et al., 2008], Procter and Gamble Pharmaceuticals Inc. [Warshakoon et al., 2006a, 2006b, 2006c, 2006d], and other teams [Nangaku et al., 2007]); and a cell-based screen using HRE-luciferase reporter construct used by a number of labs including our own (Ratan et al., Priority: 21.10.2005).

High throughput screening for PHD inhibitors using an enzyme assay is a challenge both in terms of the enzyme source and the assay format. The enzymatic activity and stability of purified PHD is very low, and enzyme assays suitable for high content screening require large quantities of recombinant enzyme supplemented with iron. One of challenges in the search for selective HIF PHD inhibitors or other regulators of HIF stability is to discriminate between nonspecific iron chelation in solution and specific iron chelation inside the active center of the PHD enzyme. The apparent iron binding constants for the 7-branched oxyquinolines identified herein (Table 1) are much lower than IC_{50} reported for 7-linear 8-hydroxyquinoline derivatives (3-10 μM) in the PHD2 in vitro assay (Warshakoon et al., 2006d), which may reflect the use of excess iron in the in vitro assay mixture as

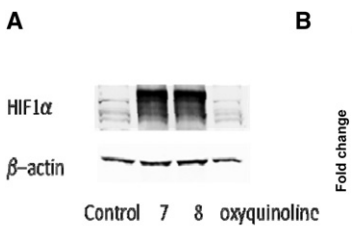

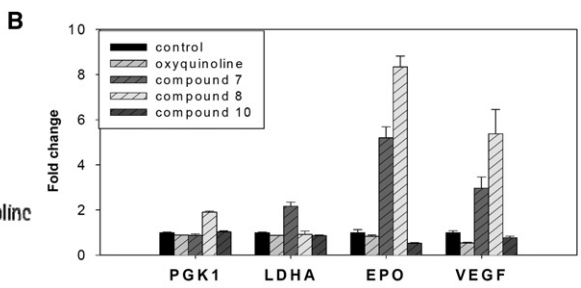

Figure 5. Upregulation of HIF1α and HIF-Regulated Human Genes

Upregulation of HIF1α (A) and HIF-regulated human genes (e.g. *EPO*, *VEGF*, *PGK1*, *LDHA*) (B) upon 3 hr treatment of neuroblastoma cells with 5 μM inhibitor (**7** and **8** as positive hits, oxyquinoline and **10** as negative hits, control with no inhibitor added). All values are presented as mean ± SEM. All compounds used have comparable cell permeability as judged by kinetics of reporter activation shown in Figure S4.

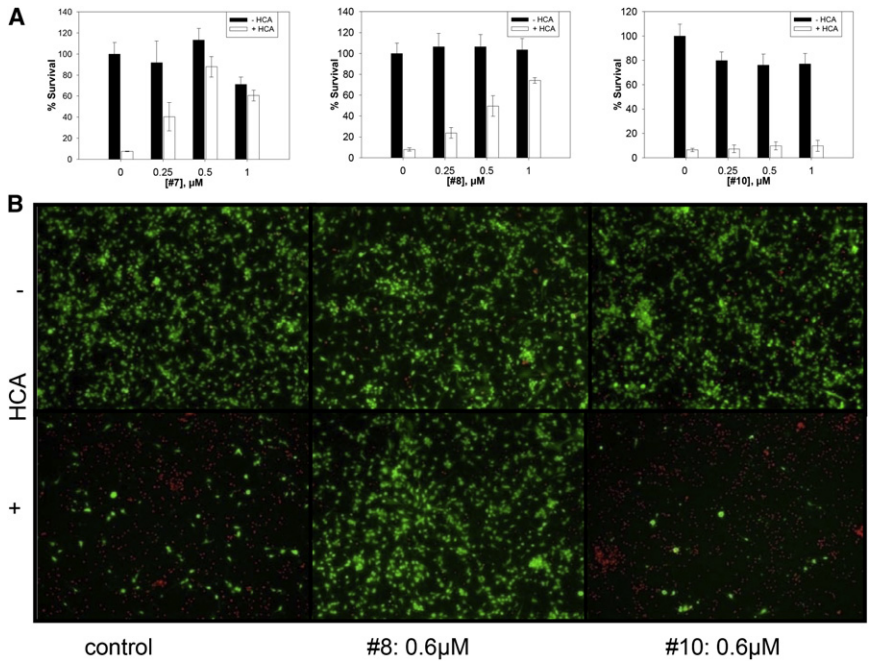

Figure 6. Neuroprotection Effects of Best Branched Oxyquinoline Hits (7,8) in Comparison with a Poor Hit from the Same Group (10) in Oxidative Stress (HCA) Model

(A) Concentration titration for (**7**,**8** and **10**).

(B) Photographs of viability test for 0.6 μM for (**8**) and (**10**). All values are presented as mean ± SEM. See Figure S5 for discussion of specificity of compounds effects.

compared with our cell-based assay. Given the nonphysiological conditions under which screening for inhibitors occurs with recombinant PHD2, it is not surprising that the IC_{50} value determined in the enzyme in vitro assay did not correlate with the IC_{50} for VEGF activation reported in the same study (Warshakoon et al., 2006d). Another limitation is the use of a 19-mer HIF peptide, whose affinity for the HIF PHDs is orders of magnitude lesser than the full-length protein. So far only Amgen team used recombinant HIF protein in HTS of their internal collection, although again they had been varying the concentration of αKG, not HIF, when determining the inhibition constant for their best hit (Tegley et al., 2008). Current studies are underway to establish the affinity of our ODD-luciferase construct (containing 128 amino acids from HIF-1α) for the HIF PHDs. A negative consequence of the test tube strategy is the assay format is more likely to yield inhibitors competitive with respect to αKG than those competing with HIF itself. The recently reported crystal structure of PHD2 with a 17-mer HIF peptide (Chowdhury et al., 2009) shows no active-site water displacement, which appears to be a mandatory requirement for the initiation of the catalytic cycle (see p.277 in Solomon et al., 2000, and Price et al., 2005). Given these biases, it is not surprising that all PHD inhibitors developed using the recombinant enzyme explored only the αKG-binding motif inside PHD2 active site and had a carboxyl group interacting with Arg-383 in addition to a clearly defined iron-binding motif (Tegley et al., 2008; Warshakoon et al., 2006a, 2006b, 2006c, 2006d; Ivan et al., 2002).

The cell-based assay with HRE-luc reporter system, a promoter-reporter construct that contained 68 bp of a known hypoxia and HIF-1 regulated gene, enolase, containing a wild-type HRE (5′-RCTGT-3′), is a widely used approach for screening of HIF activators with diverse mechanisms of action (Semenza et al., 1996). A reporter system is based on transfected immortalized hippocampal neuroblast cell line (HT22) and allows screening for a broad spectrum of compounds that include activators of HIF transcription, activators of HIF binding to HRE, and effectors of HIF protein stability (PHD inhibitors, pVHL, and proteasome inhibitors). The manual screen of Spectrum library performed in this laboratory using HRE-luc/HT22 line took half a year and resulted in 43 hits. However, in our hands, the cell line's response to positive controls decreases after seven passages, making the system not suitable for a robotic HTS on 384-well plates.

Taking into account the low specific activity of recombinant enzymes, and the inadequacy of interpretation of the inhibition constant generated using different types of enzyme in vitro assays, we developed a cell-based reporter system for HTS of ODD-luc stability, a variant of the cell-based "capture" assay, and accomplished a screen of 85,000 structurally diverse compounds in less than a month. We identified a novel, previously unknown structural motif in the group of catechol-type and oxyquinoline hits that suggests specific recognition by PHD among other αKG-dependent Fe-dioxygenases. Comparison of crystal structures of PHD2 (Figure S5A) and FIH (Figure S5) shows the difference in access to the active sites: PHD2 allows sliding of the αKG mimic into the active site, leaving the branched portion outside, whereas FIH does not. Analysis of docking modes for best hits from our HTS into the available crystal structures of αKG-dependent Fe-dioxygenases, e.g., FIH (Figure S5C), HIF PHD2 (Figure 4C), and jumonji histone demethylase (Figure S5D), demonstrates that newly identified branched motifs provide specificity for HIF PHD by exploring the active site entrance which significantly differs from those of the other enzymes of this class. In addition, these branched inhibitors did not fit into the active center of lipoxygenase-12 (Figures S5E-S5G), the enzyme directly implicated into the survival mechanism in glutathione-depletion HCA model (Ratan et al., 2002). Although future studies will examine these modeling predictions experimentally, the presence of the newly identified branched motif appears to increase the likelihood of the inhibitor specificity for HIF PHD. For the future, it is the branched motif that holds the promise to discriminate between different PHD isoforms: construction of novel mutant reporter lines that are currently in progress in this laboratory will not only allow us to answer questions regarding the specificity of PHD isoforms for regulating HIF under conditions close to physiological, but also can provide a mechanism for intelligent design of novel inhibitors that may discriminate between different PHD forms.

SIGNIFICANCE

Brain ischemia underlies many nervous system disorders triggering a cascade of events that induce acute and delayed changes resulting in disability and cognitive decline. Over the past decade, cell adaptation to hypoxia has emerged as an active process. Although the panoply of mechanisms involved in hypoxic preconditioning are incompletely understood, the discovery of HIF opened new horizons for the treatment of ischemia. Recent evidence strongly suggests that HIF PHDs and FIH are important targets for medical intervention: small molecules that inhibit HIF PHDs are the focus of drug development efforts directed toward the treatment of ischemia in many organs, including the muscle, heart, and brain. The validation of the reporter construct performed in this work shows the cell-based system capacity both for substrate specificity studies and for quantitative inhibition studies: (1) the mutational analysis presents a novel approach to study sequence-specificity of PHDs, and (2) quantitative treatment of reporter activation kinetics permits direct calculation of an apparent inhibition constant instead of IC_{50}. The results presented here are the first comprehensive report on HTS for HIF activators/HIF PHD inhibitors under the conditions most closely resembling physiological ones. We found a novel, previously undescribed branching motif adjacent to iron-binding ligands in the group of catechol-type and oxyquinoline hits that warrants specific recognition by PHD among other αKG dependent Fe-dioxygenases due to the structural constraints. The biological effects of newly identified branched hits were in accord with their rating in HTS. Altogether these findings validate a novel HTS for small molecules that can modulate hypoxic adaptation.

EXPERIMENTAL PROCEDURES

Materials

Cell Lines

Human neuroblastoma SH-SY5Y cells were transfected with 1 μg pcDNA3-ODDLUC8 or mutant variants of this plasmid by using Lipofectamine™ 2000 (Invitrogen). Transfected cell were grown in the presence of 500 μg/ml Geneticin (GIBCO-Invitrogen) on DMEM/F12+GlitaMAX (Dulbecco's modified Eagle medium Nutrient Mixture F-12 (Ham)(1:1) 1X, GIBCO 10565) medium.

Reporter Plasmid Construction and Mutagenesis

The ODDLUC encoded plasmid pcDNA3-ODDLUC8 was constructed as described previously (Safran et al., 2006). This plasmid was used as a template to introduce amino acid substitutions into the PYIP (564-567 aa) region of HIF-ODD fragment that was suggested to determine enzyme-specific interaction of HIF-1α to three isoforms of HIF PHDs (Safran et al., 2006). The plasmids pPAIP, pPYIA, and pAYIA were obtained from pcDNA3-ODDLUC8 using QuikChange Multi Site-Directed Mutagenesis kit (Agilent Technology) to introduce the corresponding mutations: Tyr565Ala, Pro567Ala, and Pro564Ala/Pro567Ala. pAYIA was used as a control line.

Methods

HTS Optimization and SAR Analysis

The assay was optimized for HTS format to provide Z values above 0.7. SH-SY5Y-ODD-luc cells were plated into 384 well, white, flat-bottom plates at 7000 cell/well in 30 μl serum and incubated overnight at 37°C, 5% CO_2. The next day compounds were added to a final concentration of 10 μM, plates were incubated for 3 hr at 37°C, and luciferase activity was measured using SteadyGlo™ reagent (Promega). Each plate had two internal standards, ciclopirox (100%) and DMSO (0%). The reporter activation (%) was calculated as a ratio $(L–L_{DMSO})/(L_{ciclopirox}-L_{DMSO})$. Hits were defined as those greater than 25%. HTS of 85,000 compounds was performed at Rockefeller HTS Resource Center. A total of 295 hits from the initial screen have been tested in quadruplicate, and 160 were confirmed. Classification into ten structural clusters has been done manually; 25 hits were singletons.

Extended SAR Analysis

Oxyquinolines were purchased from ChemDiv (San Diego, CA) and tested in 96-format plates with varied concentrations of an inhibitor (0.05-15 μM). Cells were plated at the density of 30,000 cell per well using a WellMate multichannel dispenser from Matrix (Thermo Fisher Scientific) and grown overnight on DMEM/F12+GlitaMAX (100 μl per well). Then the inhibitor was added, and the plates were incubated for a fixed time interval; the medium was removed, cells were lysed, and luciferase activity was measured on a luminometer platereader Lmax11^{384} (Molecular Devices) with BrightGlo™ reagent (Promega). The reporter activation was normalized to the background luminescence.

Kinetics of reporter activation were measured by adding varied fixed concentrations of an inhibitor at different time points followed by simultaneous cell lysis and activity measurement in the whole 96-well plate; this assay format minimizes experimental error originated from the well-known instability of luciferase reagent.

HIF Immunoblot

After 3 hr of 5 μM drug treatment, cells were scraped in iced cold PBS and centrifuged at 1,000 x *g* per 5 min. The pellet was used for nuclear extract preparation with the NE-PER Nuclear and Cytoplasmic Extraction kit (Pierce). After SDS-PAGE followed by transfer to a nitrocellulose membrane, the latter was incubated overnight at 4°C with primary polyclonal antibody against HIF-1α (Upstate) and monoclonal antibody against β-actin (Sigma) (dilution 1:250 and 1:5000, respectively, in Odyssey Blocking Buffer). Secondary fluorophore conjugated Odyssey IRDye-680 and IRD-800 antibodies (LI-COR Biosciences) were added at 1:20,000 in Odyssey Blocking Buffer, and incubated for 1h at RT. Immunoreactive proteins were detected using Odyssey IR-imaging system (LI-COR Biosciences).

Real-Time Polymerase Chain Reaction

Total RNA was isolated from SH-SY5Y cells by using NucleoSpin RNAII kit (Macherey-Nagel) and was used for cDNA synthesis by SuperScript III First-Strand Synthesis System for RT-PCR (Invitrogen). Quantitative real-time PCR analyses of human PHD1,2,3, LDHA, PKG1 and EPO were performed by using the corresponding primers and probe set from Applied Biosystems on the ABI 7500 Fast Real Time PCR TaqMan system (Applied Biosystems). GAPDH was used for normalization.

Cell Death and Viability Assays

Primary neuronal cultures were prepared from the forebrains of Sprague-Dawley rat embryos (E17) and plated on 96-well plates at a 10^6 cells/ml density. After 16 hr, cells were rinsed with warm phosphate-buffered saline and then placed in minimum essential medium (Life Technologies) containing 5 mM HCA in the presence of oxyquinolines (0.25-2 μM). Cells were incubated for 24 hr or longer to see 90% cell death in HCA-treated controls. Viability was assessed by the MTT (4,5-dimethylthiazol-2-yl)-2,5-diphenyltetrazolium bromide) assay (Mosmann, 1983).

Iron-Binding Properties of Oxyquinolines

The iron chelation ability is determined by displacement of calcein from its complex with iron monitored by fluorescence (excitation 490 nm, emission 523 nm, cutoff 515 nm) on a Spectramax M5^e platereader (Molecular Devices). The apparent binding constant for calcein (ca. 50 nM) was determined from Fe titration curve for 1 μM calcein in 5 mM Tris-HCl buffer (pH 7.5). The ratio between the iron binding constant for calcein and a particular compound K_Q/K_{Ca} was estimated by fitting the titration curve into the dependence of $[Fe]_o$ versus Y, where $Y = [Ca\text{-}Fe]/[Ca]$ is a ratio of calcein-bound Fe to free (fluorescent) calcein:

$$[Fe]o = K_{Ca}Y + [Ca]oY/(Y+1) + [Q]oY/(Y + K_Q/K_{Ca}). \quad (4)$$

The association rate constant was determined as the second order rate constant for calcein displacement from its complex with iron (1 μM:1 μM) upon addition of an oxyquinoline (5-20 μM) calculated from the slope of a linear plot of the initial rate of calcein release versus the concentration of oxyquinoline added. All experiments were performed in triplicates or more. All values are presented as mean and standard error of the mean (± SEM).

Computer Modeling

Docking experiments were performed using the CDOCKER algorithm (Wu et al., 2003) as implemented in the Discovery Studio 2.5 software suite (Accelrys, San Diego, CA), followed by force-field minimization and binding energy calculations using the PHD2 crystal structure with the bound inhibitor (2G19.pdb) as the starting template structure. Preparation of the receptor was done by running a protein check and identifying all the elements of the structure. It was noted that there were amino acids missing on the N terminus and C terminus, however these were not in close proximity to the binding site and therefore there was no need to add them to the structure. Force-field minimization was carried out using the molecular mechanics algorithm CHARMm (Brooks et al., 1983) as implemented in Discovery Studio 2.5.

SUPPLEMENTAL INFORMATION

Supplemental Information includes five figures and one table and can be found with this article online at doi:10.1016/j.chembiol.2010.03.008.

ACKNOWLEDGMENTS

We thank Ronald Realubit, BS, for his help with HTS, and Dmitry Hushpulian, PhD, for introducing into various docking programs and help with alignment and docking. This work was funded by the Winifred Masterson Burke Relief Foundation, the Adelson Foundation for Neurorehabilitation and Repair, and NYS DOH Center of Research Excellence # CO19772. I.N.G was supported by NIH grant #1R43CA133985-01.

Received: December 18, 2009
Revised: February 26, 2010
Accepted: March 9, 2010
Published: April 22, 2010

REFERENCES

Adlard, P.A., Cherny, R.A., Finkelstein, D.I., Gautier, E., Robb, E., Cortes, M., Volitakis, I., Liu, X., Smith, J.P., Perez, K., et al. (2008). Rapid restoration of cognition in Alzheimer's transgenic mice with 8-hydroxy quinoline analogs is associated with decreased interstitial Abeta. Neuron *59*, 43–55.

Almstead, J.-I.K., Izzo, N.J., Jones, D.R., and Kawamoto, R.M. (2002) Medicinal uses of hydrazones issued. US Patent 6660737.

Aminova, L., Siddiq, A., and Ratan, R.R. (2008). Antioxidants, HIF prolyl hydroxylase inhibitors or short interfering RNAs to BNIP3 or PUMA, can prevent prodeath effect of the transcriptional activator, HIF-1alpha, in a mouse hippocampal neuronal line. Antioxid. Redox Signal *10*, 1989–1998.

Asikainen, T.M., Ahmad, A., Schneider, B.K., Ho, W.B., Arend, M., Brenner, M., Gunzler, V., and White, C.W. (2005). Stimulation of HIF-1alpha, HIF-2alpha, and VEGF by prolyl 4-hydroxylase inhibition in human lung endothelial and epithelial cells. Free Radic. Biol. Med. *38*, 1002–1013.

Baranova, O., Miranda, L.F., Pichiule, P., Dragatsis, I., Johnson, R.S., and Chavez, J.C. (2007). Neuron-specific inactivation of the hypoxia inducible factor 1 alpha increases brain injury in a mouse model of transient focal cerebral ischemia. J. Neurosci. *27*, 6320–6332.

Brooks, B.R., Bruccoleri, R.E., Olafson, B.D., States, D.J., Swaminathan, S., and Karplus, M. (1983). CHARMM: A program for macromolecular energy minimization and dynamics calculations. J. Comput. Chem. *4*, 187–217.

Bruick, R.K., and McKnight, S.L. (2001). A conserved family of prolyl-4-hydroxylases that modify HIF. Science *294*, 1337–1340.

Chan, D.A., Sutphin, P.D., Yen, S.E., and Giaccia, A.J. (2005). Coordinate regulation of the oxygen-dependent degradation domains of hypoxia-inducible factor 1 alpha. Mol. Cell. Biol. *25*, 6415–6426.

Cho, H., Park, H., and Yang, E.G. (2005). A fluorescence polarization-based interaction assay for hypoxia-inducible factor prolyl hydroxylases. Biochem. Biophys. Res. Commun. *337*, 275–280.

Choi, S.M., Choi, K.O., Park, Y.K., Cho, H., Yang, E.G., and Park, H. (2006). Clioquinol, a Cu(II)/Zn(II) chelator, inhibits both ubiquitination and asparagine hydroxylation of hypoxia-inducible factor-1alpha, leading to expression of vascular endothelial growth factor and erythropoietin in normoxic cells. J. Biol. Chem. *281*, 34056–34063.

Chowdhury, R., McDonough, M.A., Mecinovic, J., Loenarz, C., Flashman, E., Hewitson, K.S., Domene, C., and Schofield, C.J. (2009). Structural basis for binding of hypoxia-inducible factor to the oxygen-sensing prolyl hydroxylases. Structure *17*, 981–989.

Dao, J.H., Kurzeja, R.J., Morachis, J.M., Veith, H., Lewis, J., Yu, V., Tegley, C.M., and Tagari, P. (2009). Kinetic characterization and identification of a novel inhibitor of hypoxia-inducible factor prolyl hydroxylase 2 using a time-resolved fluorescence resonance energy transfer-based assay technology. Anal. Biochem. *384*, 213–223.

Hewitson, K.S., Schofield, C.J., and Ratcliffe, P.J. (2007). Hypoxia-inducible factor prolyl-hydroxylase: purification and assays of PHD2. Methods Enzymol. *435*, 25–42.

Hirota, K., and Semenza, G.L. (2005). Regulation of hypoxia-inducible factor 1 by prolyl and asparaginyl hydroxylases. Biochem. Biophys. Res. Commun. *338*, 610–616.

Ivan, M., Haberberger, T., Gervasi, D.C., et al. (2002). Biochemical purification and pharmacological inhibition of a mammalian prolyl hydroxylase acting on hypoxia-inducible factor. Proc. Natl. Acad. Sci. USA *99*, 13459–13464.

Jaakkola, P., Mole, D.R., Tian, Y.M., et al. (2001). Targeting of HIF-alpha to the von Hippel-Lindau ubiquitylation complex by O2-regulated prolyl hydroxylation. Science *292*, 468–472.

Jeon, H., Kim, H., Choi, D., Kim, D., Park, S.Y., Kim, Y.J., Kim, Y.M., and Jung, Y. (2007). Quercetin activates an angiogenic pathway, hypoxia inducible factor (HIF)-1-vascular endothelial growth factor, by inhibiting HIF-prolyl hydroxylase: a structural analysis of quercetin for inhibiting HIF-prolyl hydroxylase. Mol. Pharmacol. *71*, 1676–1684.

Kaelin, W.G., Jr. (2005). The von Hippel-Lindau protein, HIF hydroxylation, and oxygen sensing. Biochem. Biophys. Res. Commun. *338*, 627–638.

Kaur, D., Yantiri, F., Rajagopalan, S., et al. (2003). Genetic or pharmacological iron chelation prevents MPTP-induced neurotoxicity in vivo: a novel therapy for Parkinson's disease. Neuron *37*, 899–909.

Kikuchi, K., Kawahara, K., Tancharoen, S., et al. (2009a). The free radical scavenger edaravone rescues rats from cerebral infarction by attenuating the release of high-mobility group box-1 in neuronal cells. J. Pharmacol. Exp. Ther. *329*, 865–874.

Kikuchi, K., Tancharoen, S., Matsuda, F., et al. (2009b). Edaravone attenuates cerebral ischemic injury by suppressing aquaporin-4. Biochem. Biophys. Res. Commun. *390*, 1121–1125.

Knowles, H.J., Tian, Y.M., Mole, D.R., and Harris, A.L. (2004). Novel mechanism of action for hydralazine: induction of hypoxia-inducible factor-1alpha, vascular endothelial growth factor, and angiogenesis by inhibition of prolyl hydroxylases. Circ. Res. *95*, 162–169.

Koivunen, P., Hirsila, M., Kivirikko, K.I., and Myllyharju, J. (2006). The length of peptide substrates has a marked effect on hydroxylation by the hypoxia-inducible factor prolyl 4-hydroxylases. J. Biol. Chem. *281*, 28712–28720.

Landazuri, M.O., Vara-Vega, A., Viton, M., Cuevas, Y., and del Peso, L. (2006). Analysis of HIF-prolyl hydroxylases binding to substrates. Biochem. Biophys. Res. Commun. *351*, 313–320.

Lando, D., Peet, D.J., Whelan, D.A., Gorman, J.J., and Whitelaw, M.L. (2002). Asparagine hydroxylation of the HIF transactivation domain a hypoxic switch. Science *295*, 858–861.

Liu, X.B., Wang, J.A., Ogle, M.E., and Wei, L. (2009). Prolyl hydroxylase inhibitor dimethyloxalylglycine enhances mesenchymal stem cell survival. J. Cell. Biochem. *106*, 903–911.

Lomb, D.J., Desouza, L.A., Franklin, J.L., and Freeman, R.S. (2009). Prolyl hydroxylase inhibitors depend on extracellular glucose and hypoxia-inducible factor (HIF)-2alpha to inhibit cell death caused by nerve growth factor (NGF) deprivation: evidence that HIF-2alpha has a role in NGF-promoted survival of sympathetic neurons. Mol. Pharmacol. *75*, 1198–1209.

Mabjeesh, N.J., Willard, M.T., Harris, W.B., Sun, H.Y., Wang, R., Zhong, H., Umbreit, J.N., and Simons, J.W. (2003). Dibenzoylmethane, a natural dietary

compound, induces HIF-1 alpha and increases expression of VEGF. Biochem. Biophys. Res. Commun. *303*, 279–286.

Michels, C., Dorai, T., Chander, P., Choudhury, M., and Grasso, M. (2009). Hypoxic pre-conditioning in a rat renal ischemia model: an evaluation of the use of hydralazine. World J. Urol.

Mikhaylova, O., Ignacak, M.L., Barankiewicz, T.J., Harbaugh, S.V., Yi, Y., Maxwell, P.H., Schneider, M., Van Geyte, K., Carmeliet, P., Revelo, M.P., et al. (2008). The von Hippel-Lindau tumor suppressor protein and Egl-9-Type proline hydroxylases regulate the large subunit of RNA polymerase II in response to oxidative stress. Mol. Cell. Biol. *28*, 2701–2717.

Mosmann, T. (1983). Rapid colorimetric assay for cellular growth and survival: application to proliferation and cytotoxicity assays. J. Immunol. Methods *65*, 55–63.

Nangaku, M., Izuhara, Y., Takizawa, S., Yamashita, T., Fujii-Kuriyama, Y., Ohneda, O., Yamamoto, M., van Ypersele de Strihou, C., Hirayama, N., and Miyata, T. (2007). A novel class of prolyl hydroxylase inhibitors induces angiogenesis and exerts organ protection against ischemia. Arterioscler. Thromb. Vasc. Biol. *27*, 2548–2554.

Philipp, S., Cui, L., Ludolph, B., Kelm, M., Schulz, R., Cohen, M.V., and Downey, J.M. (2006). Desferoxamine and ethyl-3,4-dihydroxybenzoate protect myocardium by activating NOS and generating mitochondrial ROS. Am. J. Physiol. Heart Circ. Physiol. *290*, H450–H457.

Price, J.C., Barr, E.W., Hoffart, L.M., Krebs, C., and Bollinger, J.M., Jr. (2005). Kinetic dissection of the catalytic mechanism of taurine:alpha-ketoglutarate dioxygenase (TauD) from Escherichia coli. Biochemistry *44*, 8138–8147.

Ratan, R.R., Siddiq, A., and Chavez, J. (2005) Compounds for enhancing hypoxia inducible factor activity and methods of use. WO/2007/048004; 60/729,059.

Ratan, R.R., Ryu, H., Lee, J., Mwidau, A., and Neve, R.L. (2002). In vitro model of oxidative stress in cortical neurons. Methods Enzymol. *352*, 183–190.

Safran, M., Kim, W.Y., O'Connell, F., Flippin, L., Gunzler, V., Horner, J.W., Depinho, R.A., and Kaelin, W.G., Jr. (2006). Mouse model for noninvasive imaging of HIF prolyl hydroxylase activity: assessment of an oral agent that stimulates erythropoietin production. Proc. Natl. Acad. Sci. USA *103*, 105–110.

Semenza, G.L., Jiang, B.H., Leung, S.W., Passantino, R., Concordet, J.P., Maire, P., and Giallongo, A. (1996). Hypoxia response elements in the aldolase A, enolase 1, and lactate dehydrogenase A gene promoters contain essential binding sites for hypoxia-inducible factor 1. J. Biol. Chem. *271*, 32529–32537.

Siddiq, A., Ayoub, I.A., Chavez, J.C., Aminova, L., Shah, S., LaManna, J.C., Patton, S.M., Connor, J.R., Cherny, R.A., Volitakis, I., et al. (2005). Hypoxia-inducible factor prolyl 4-hydroxylase inhibition. A target for neuroprotection in the central nervous system. J. Biol. Chem. *280*, 41732–41743.

Siddiq, A., Aminova, L.R., Troy, C.M., Suh, K., Messer, Z., Semenza, G.L., and Ratan, R.R. (2009). Selective inhibition of hypoxia-inducible factor (HIF) prolyl-hydroxylase 1 mediates neuroprotection against normoxic oxidative death via HIF- and CREB-independent pathways. J. Neurosci. *29*, 8828–8838.

Solomon, E.I., Brunold, T.C., Davis, M.I., Kemsley, J.N., Lee, S.K., Lehnert, N., Neese, F., Skulan, A.J., Yang, Y.S., and Zhou, J. (2000). Geometric and electronic structure/function correlations in non-heme iron enzymes. Chem. Rev. *100*, 235–350.

Tegley, C.M., Viswanadhan, V.N., Biswas, K., Frohn, M.J., Peterkin, T.A., Chang, C., Bürli, R.W., Dao, J.H., Veith, H., Rogers, N., et al. (2008). Discovery of novel hydroxy-thiazoles as HIF-alpha prolyl hydroxylase inhibitors: SAR, synthesis, and modeling evaluation. Bioorg. Med. Chem. Lett. *18*, 3925–3928.

Tuckerman, J.R., Zhao, Y., Hewitson, K.S., Tian, Y.M., Pugh, C.W., Ratcliffe, P.J., and Mole, D.R. (2004). Determination and comparison of specific activity of the HIF-prolyl hydroxylases. FEBS Lett. *576*, 145–150.

Villar, D., Vara-Vega, A., Landazuri, M.O., and Del Peso, L. (2007). Identification of a region on hypoxia-inducible-factor prolyl 4-hydroxylases that determines their specificity for the oxygen degradation domains. Biochem. J. *408*, 231–240.

Wang, G.L., and Semenza, G.L. (1995). Purification and characterization of hypoxia-inducible factor 1. J. Biol. Chem. *270*, 1230–1237.

Wang, G.L., Jiang, B.H., Rue, E.A., and Semenza, G.L. (1995). Hypoxia-inducible factor 1 is a basic-helix-loop-helix-PAS heterodimer regulated by cellular O2 tension. Proc. Natl. Acad. Sci. USA *92*, 5510–5514.

Warshakoon, N.C., Wu, S., Boyer, A., Kawamoto, R., Renock, S., Xu, K., Pokross, M., Evdokimov, A.G., Zhou, S., et al. (2006a). Design and synthesis of a series of novel pyrazolopyridines as HIF-1alpha prolyl hydroxylase inhibitors. Bioorg. Med. Chem. Lett. *16*, 5687–5690.

Warshakoon, N.C., Wu, S., Boyer, A., Kawamoto, R., Sheville, J., Bhatt, R.T., Renock, S., Xu, K., Pokross, M., Zhou, S., et al. (2006b). Design and synthesis of substituted pyridine derivatives as HIF-1alpha prolyl hydroxylase inhibitors. Bioorg. Med. Chem. Lett. *16*, 5616–5620.

Warshakoon, N.C., Wu, S., Boyer, A., Kawamoto, R., Sheville, J., Renock, S., Xu, K., Pokross, M., Evdokimov, A.G., Walter, R., and Mekel, M. (2006c). A novel series of imidazo[1,2-a]pyridine derivatives as HIF-1alpha prolyl hydroxylase inhibitors. Bioorg. Med. Chem. Lett. *16*, 5598–5601.

Warshakoon, N.C., Wu, S., Boyer, A., Kawamoto, R., Sheville, J., Renock, S., Xu, K., Pokross, M., Zhou, S., Winter, C., et al. (2006d). Structure-based design, synthesis, and SAR evaluation of a new series of 8-hydroxyquinolines as HIF-1alpha prolyl hydroxylase inhibitors. Bioorg. Med. Chem. Lett. *16*, 5517–5522.

Wilson, W.J., and Poellinger, L. (2002). The dietary flavonoid quercetin modulates HIF-1 alpha activity in endothelial cells. Biochem. Biophys. Res. Commun. *293*, 446–450.

Wu, G., Robertson, D.H., Brooks, C.L., 3rd, and Vieth, M. (2003). Detailed analysis of grid-based molecular docking: A case study of CDOCKER-A CHARMm-based MD docking algorithm. J. Comput. Chem. *24*, 1549–1562.

Xie, L., Xiao, K., Whalen, E.J., Forrester, M.T., Freeman, R.S., Fong, G., Gygi, S.P., Lefkowitz, R.J., and Stamler, J.S. (2009). Oxygen-regulated 2-adrenergic receptor hydroxylation by EGLN3 and ubiquitylation by pVHL. Sci. Signal *2*, 1–10.

Zhang, C.P., Zhu, L.L., Zhao, T., Zhao, H., Huang, X., Ma, X., Wang, H., and Fan, M. (2006). Characteristics of neural stem cells expanded in lowered oxygen and the potential role of hypoxia-inducible factor-1Alpha. Neurosignals *15*, 259–265.